Numerical Evaluation of Design Rules for Non-Breaking Wave Loads on Vertical Walls

van Vledder, Gerbrant; Hofland, Bas; Tuin, Henry; van Maris, Bob

DOI
10.18451/978-3-939230-64-9_076

Publication date
2019

Document Version
Final published version

Published in
Coastal Structures 2019

Citation (APA)
van Vledder, G., Hofland, B., Tuin, H., & van Maris, B. (2019). Numerical Evaluation of Design Rules for Non-Breaking Wave Loads on Vertical Walls. In N. Goseberg, & T. Schlurmann (Eds.), *Coastal Structures 2019* Bundesanstalt für Wasserbau. https://doi.org/10.18451/978-3-939230-64-9_076

Conference Paper, Published Version

van Vledder, Gerbrant; Hofland, Bas; Tuin, Henry; van Maris, Bob

Numerical Evaluation of Design Rules for Non-Breaking Wave Loads on Vertical Walls

Coastal Structures 2019 - Nils Goseberg, Torsten Schlurmann (eds) - © 2019 Bundesanstalt für Wasserbau
ISBN 978-3-939230-64-9 (Online) - DOI: 10.18451/978-3-939230-64-9_076

Numerical Evaluation of Design Rules for Non-Breaking Wave Loads on Vertical Walls

G. Ph. van Vledder[1,2], B. Hofland[1], H. Tuin[3] & B. van Maris[1]
[1]*Faculty of Civil Engineering and Geosciences, Delft University of Technology, P.O. Box 5048, 2600 GA Delft, The Netherlands*
[2]*Van Vledder Consulting, Olst, The Netherlands*
[3]*Arcadis, Amersfoort, The Netherlands*

Abstract: This paper describes a numerical evaluation of design rules for the determination of wave loads of non-breaking waves on vertical structures. Design guidelines were proposed by Sainflou (1928) and Goda (1974). These guidelines use geometric parameters of the structure, an incident wave height and a wave period. In practice (cf. CERC, 1984), a Rayleigh distribution of individual wave heights is assumed to determine the design wave height in an irregular wave field. Their reliability and range of applicability are poorly known, especially when the incident wave condition consists of a mixed sea state, like a local wind sea and a low-frequency (swell) component. To validate the above described design methods, we applied the non-hydrostatic numerical wave model SWASH to simulate wave loading on a rigid vertical wall for single and mixed sea states. In addition, we compared the results with linear wave theory and the spectral response approach using transfer functions based on linear wave theory.

Keywords: Wave load, vertical structures, Goda, Sainflou, SWASH, force spectrum, linear wave theory

1 Introduction

Hydraulic structures with a vertical wall such as locks and storm surge barriers can be loaded by waves. The load of non-breaking waves on vertical walls can be estimated by means of different design methods. The simplest one being linear wave theory applied to the design wave to infer the vertical pressure distribution. More advanced methods are the guidelines proposed by Sainflou (1928) and Goda (1974). These design formulae are based on geometric parameters, a design wave height and a design wave period. The design wave height is found by extrapolation of the significant wave height with a design factor assuming a Rayleigh distribution of wave heights and a certain probability of occurrence. Unfortunately, different versions of design formulae appear and the accounted design probability is not explicitly given. This results in ambiguity when determining the horizontal wave force.

A common method to determine wave loads for irregular incident waves is based on a spectral calculation which transfers the incident wave spectrum to a force spectrum using a response function based on the linear wave theory (cf. Holthuijsen, 2007). This approach works well in case of unimodal spectra, but its applicability is unknown in case the incident wave spectrum consists of a bimodal spectrum. Such conditions were encountered in the design of a new lock in the Port of IJmuiden, the Netherlands (Tuin et al., 2018). The low frequency wave component with limited wave energy (3% of total energy) results in a relatively large peak (20% to 30% of total force) in the force spectrum. This raises the question whether formulas given in guidelines account for this.

The different design rules and their applicability to bimodal sea-states, were studied by means of numerical simulations with the non-hydrostatic numerical wave model SWASH (Zijlema et al., 2011). It is a time domain model able to simulate the loading of a vertical structure by irregular non-breaking incident waves, as specified by a wave spectrum. By integrating the computed time variation of the vertical pressure distribution, a direct evaluation of different design methods is possible.

The setup of comparing these design methods (design rules, spectral method and direction numerical simulation) is outlined in Figure 1. The input consists of the specification of the design condition, usually obtained from a statistical analysis of nearshore wave conditions translated to incident wave conditions in front of the structure (Tuin et al., 2018, Van Vledder, 2018) and the output consists of a design force on the vertical structure. The direct numerical evaluation using the SWASH model is indicated with the middle arrow (1). The application of the design guidelines of Sainflou and Goda, is indicated with the upper arrows (4, 5, 2), whereas the spectral calculation method is indicated with the lower arrows (3 and 6).

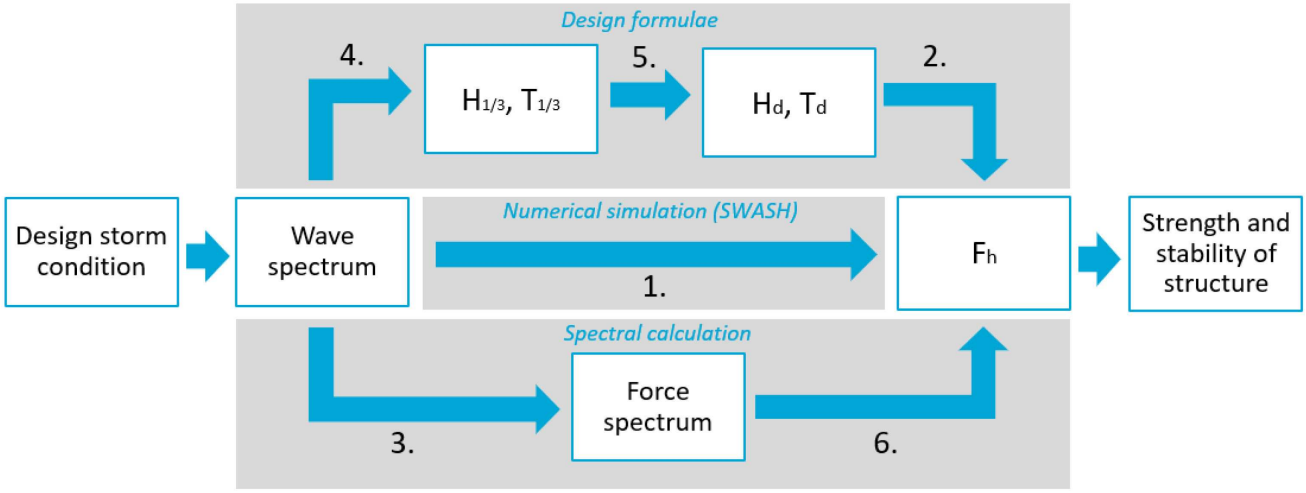

Fig. 1. The application of three categories of design methods, determining a horizontal design force, based on an incident wave spectrum. The arrows indicate the design steps that are taken under consideration (source: Van Maris, 2018).

The results in this paper are based on Van Maris (2018), in which also attention was paid to the probability density function of individual wave heights and peak pressures, as well as the increase in water level as predicted by the Sainflou method. These subjects will be reported elsewhere.

The outline of this paper is as follows. Section 2 provides a summary of presently used design methods as indicated in Figure 1. The setup of the numerical wave model and the analysis method are described in Section 3. Results of the numerical computations and comparison with commonly used design rules are provided in Section 4. Conclusions and recommendations are given in Section 5.

2 Summary of design methods

2.1 Pressure distribution according to linear wave theory

The determination of wave induced forces is based on the vertical integration of wave pressures on a vertical structure with a certain reflection coefficient χ. The contribution of the hydrostatic pressure is usually omitted from the design rules as they cancel out with equal water levels on both sides of the vertical structure. For a closed lock gate or barrier an additional hydrostatic pressure has to be added to the horizontal wave pressure which accounts for the maximum head difference. For a wave with amplitude a and wave number k the vertical pressure distribution can be computed from linear wave theory (LWT) as:

$$P_{top}(z) = (1+\chi)\rho g a_{inc}\left(1-\frac{z}{(1+\chi)a_{inc}}\right)$$
$$P_{sub}(z) = (1+\chi)\rho g a_{inc}\frac{\cosh\left(k(d+z)\right)}{\cosh(kd)} \quad (1)$$

in which ρ the density of water, g the gravitational acceleration, d the water depth and z the vertical coordinate. Eq. (1) makes a distinction for the area above (p_{top}) and below (p_{sub}) the still water level (SWL). As linear wave theory does not account for the pressure distribution above mean water level, a hydrostatic approximation is used. The wave number k is related to the wave period T and water depth d according to the linear dispersion relation. Figure 2 shows the wave induced pressure distribution for various wave periods. With increasing wave period T ($T_1<T_2<T_3$) the vertical profile becomes more and more constant as well as the related enhancement of wave pressure and resulting forces.

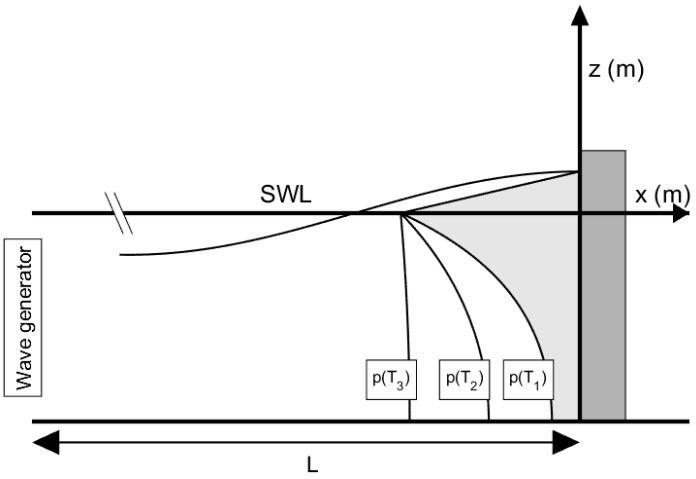

Fig. 2. Wave pressure distribution according to linear wave theory (LWT) for increasing wave period (not on scale).

For an irregular wave field, described by a wave spectrum $S_{inc}(f)$, the force spectrum $S_F(f)$ can be obtained (Holthuijsen, 2007, Tuin et al., 2018). The force spectrum $S_F(f)$ is obtained by multiplying the squared sum of two response functions with the wave variance spectrum:

$$S_F(f) = \left[R_{sub}(f) + R_{top}(f) \right]^2 S_{inc}(f) \tag{2}$$

where

f = Frequency [Hz]
$S_F(f)$ = Wave force spectrum [(kN/m)^2/Hz]
$R_{sub}(f)$ = Response function for section below SWL [kN/m^2]
$R_{top}(f)$ = Response function for section above SWL [kN/m^2]

and

$$R_{sub}(f) = \rho g \int_{-d}^{0} \frac{\cosh\left(k(f)(d+z)\right)}{\cosh\left(k(f)(-d)\right)} dz$$
$$R_{top}(f) = \frac{1}{2}\rho g a_{ref} \quad \text{(with e.g., } a_{ref} = \frac{1}{2}1.5H_{m0}\text{)} \tag{3}$$

(Note, the factor 1.5 is related to the 1% exceedance probability in the Rayleigh distribution.)

2.2 Sainflou method

Sainflou (1928) introduced a pressure formula that could be used for standing waves. This formula was directly utilized by many port engineers throughout the world. The approach of Sainflou is based on Stokes' second order wave theory and is therefore applicable to somewhat steeper waves compared to the linear wave theory.

In his method it is assumed that there is complete reflection (χ=1) and that the waves are of the non-breaking type. Figure 3 (left panel) shows the schematized piece-wise linear wave induced pressure distribution for the simplified geometry used in the present study. Sainflou includes a h_0 factor, which represents the increase in water level underneath an anti-node in a regular wave field. In addition, Sainflou (1928) introduced the factor h_0 being the additional rise in mean water level (Wiegel, 1964). Van Maris (2018) showed that this rise only occurs under the anti-node of the incident wave.

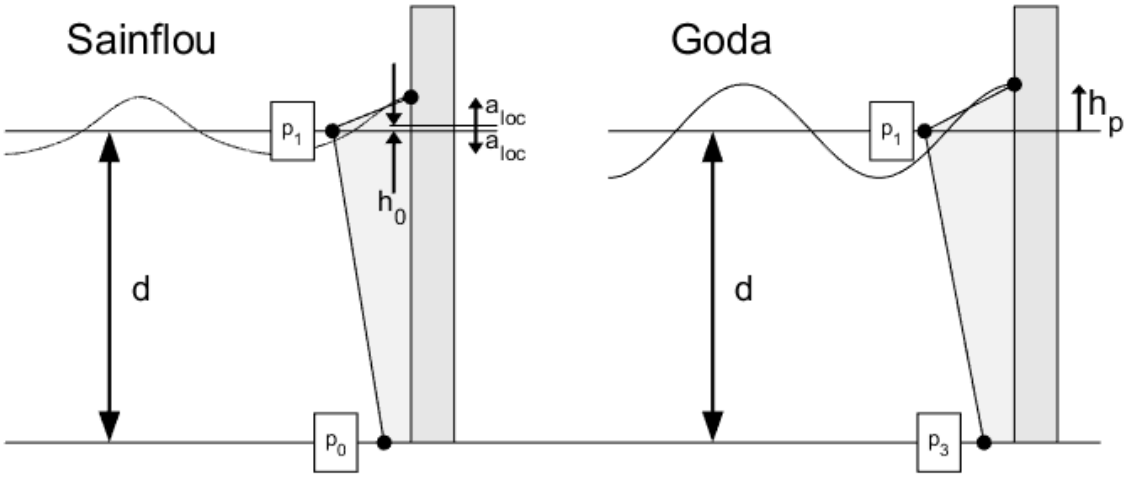

Fig. 3. Wave pressure distributions according to Sainflou (left panel) and Goda (right panel) for a simplified geometry without a foreshore slope or rubble berm, and normal wave incidence.

The characteristic pressures are computed as:

$$p_1 = \rho g\left(a_{loc} + h_0\right)$$
$$p_0 = \frac{\rho g a_{loc}}{\cosh\left(kd\right)}$$
$$h_0 = \tfrac{1}{2} k a_{loc}^2 \coth\left(kd\right) \tag{4}$$

where

p_1 = Maximum wave pressure at the level of h_0 [N/m^2]
p_0 = Wave pressure at depth d [N/m^2]
h_0 = Increase of mean water level at the wall [m]
d = Water depth directly in front of the structure [m]
a_{loc} = Amplitude of the wave directly in front of the wall (including reflection) [m]
k = Wave number of the incoming wave [m^{-1}]

For application in an irregular wave field, a local design wave amplitude a_{loc} needs to be defined. Following Dutch guidelines (TAW, 2003) we determine the local amplitude a_{loc} defined as $H_{d,loc}/2$, where the local design wave height is obtained as $H_{d,loc} = (1+\chi)H_{d,inc}$ and where $H_{d,inc}$ is chosen as 2.2 H_s. A specification of H_s as $H_{1/3}$ or H_{m0} is not made. As design wave period, the peak period T_p is chosen.

2.3 Goda method

Goda (1974) presented wave pressure formulae for the design of vertical breakwaters. The parameters Goda uses are based on a large amount of laboratory data for a wide range of boundary conditions. The final calibration of the formula was based on tests regarding damage to caisson type breakwaters on top of a berm. The Goda formulae are widely applicable in case of depth-induced breaking on the berm as well as non-breaking waves. Regardless whether the waves are breaking or non-breaking, the

pressure distribution on the vertical section is schematized trapezoidally, as shown in the right panel of Figure 3 for the simplified geometry without a berm used in this study. The omission of the berm implies that incident waves do not break. This simplification reduces the Goda formula considerably because the impact factors reduce to zero. Note: Instead of the unreflected H_{inc} in the original Goda formulae, here the local (reflected) H_{loc} is implemented. The original Goda formula includes more factors like a sloping bed, a rubble mound base, and oblique wave incidence, which makes the formula very complicated. For the simplified geometry used in this study, these factors can be omitted leading to:

$$p_1 = \left(0.6 + \tfrac{1}{2}\left[\frac{2kd}{\sinh(2kd)} \right]^2 + \frac{4d}{H_{loc}} \right) \rho g \tfrac{1}{2} H_{loc}$$

$$p_0 = \frac{p_1}{\cosh(kd)} \qquad (5)$$

$$h_p = 0.75 H_{loc}$$

where

H_d = Unreflected design wave height (according to Goda 1.8 $H_{1/3}$) [m]
p_1 = Wave pressure at still water level [N/m^2]
p_3 = Wave pressure at sea bed level [N/m^2]
h_p = Height between SWL and top of structure [m]
d = Depth directly in front of structure [m]

Goda (1974) advices $H_d = 1.8\ H_{1/3,inc}$ in case of non-breaking waves at the structure and $T_d = T_{1/3}$. The 100% wave reflectance at the wall is integrated in the formulae. Following the Dutch design rules TAW, 2003) we used $H_{d,inc} = 2.2 H_s$ and $T_d = T_{1/3}$ (similar to the Sainflou formula as adapted in the SPM). The factor 2.2 is roughly equivalent to an exceedance probability of 1:10,000 waves according to the Rayleigh distribution. For a wave record with 1,000 waves, this wave height has a 10% exceedance probability of exceedance.

3 Numerical simulations with the SWASH model

3.1 Model setup

To evaluate the various design methods, numerical simulations were carried out with the SWASH model using the schematization for the IJmuiden lock (Tuin et al., 2018; Van Maris 2018). The geometry is schematized in the 2-dimensional physical domain in Cartesian co-ordinates (x-axis, z-axis) and shown in Figure 2. It consists of a horizontal seabed with a vertical rigid structure located at x = 0 m (east boundary condition). The length of the water basin L basin in front of the vertical wall is 200 m. The downward measured water depth d is 20 m. A wave generating boundary condition is present at x=-200 m (west boundary condition) and generates irregular waves in the positive x direction. The surface elevation η is positive in the z-direction. The schematization of the wave induced pressure is indicated with the shaded area. Above SWL, the pressure distribution is approximated by assuming a hydrostatic pressure between SWL and h_p, possibly amplified with an empirical factor (Goda, 1974).

3.2 SWASH Model set-up

SWASH (acronym of Simulating WAves till SHore) is a non-hydrostatic multi-layer model developed at the TU Delft (Zijlema et al., 2011). SWASH is a phase-resolved model and is able to present the vertical pressure distribution in the time domain. Because of this, SWASH can verify both the individual wave force as well as wave heights and forces in the time domain. For this study, SWASH

4.01A is used. The offshore boundary condition is specified in terms of a wave spectrum $S(f)$ which is converted to an oscillating time dependent surface elevation η(t) using the single summation method. The vertical structure is modelled with a porosity layer (p=0.1). This low value makes the wall almost fully reflecting while enhancing numerical stability. The right boundary is modelled with a sponge layer, to absorb all incoming waves avoiding reflections. The advection approximation is strictly momentum conservative.

Before applying the SWASH model an optimization of the grid size discretization was performed. Stable results were obtained when using 6 vertical layers and grid size of Δx=0.25 m. The duration of each SWASH simulation is such that at least 1000 individual wave heights are simulated excluding the waves occurring during the spin-up time. Hereafter, the SWASH results were compared with the physical experiment by Gurhan and Unsalan (2005). Froude-scaling ($H \sim 40$ and $T \sim \sqrt{40}$) was applied to convert the 1:40 scale experiments to prototype scale. SWASH reproduced an accurate increase in wave pressure for increasing wave steepness. However, overall the SWASH simulations were a percentage of about 15% lower than the experiment. The precise origin of these differences is unknown, but they may be due to scale effects. Further experiences in SWASH showed a correlation of pressures between the simulation of steep waves in irregular wave fields and the experimental results of Gurhan and Unsalan (2005). From these observations it is concluded that SWASH is capable of simulating gentle waves. As all design methods are inter-compared in relation to the simulated conditions just in front of the vertical structure, spin-up effect near the wave generator area do not play a role in the present analysis.

3.3 Simulations

The SWASH simulations were performed using irregular incident wave conditions, for unimodal as well as bimodal wave spectra. For the present analysis the wave spectra were schematized as JONSWAP spectra (Hasselmann et al., 1973) using a peak enhancement factor of γ=3.3 for wind seas and γ=20 for swell waves. For each spectrum the wave variance m_0 is computed by integration over frequency, from which the corresponding significant wave height can be computed according to $H_{m0}=4(m_0)^{1/2}$. To determine the effect of bimodal spectra on the design wave forces two dimensionless parameters are defined based on the ratio M_{Sw} of wave variances of the wind sea and swell part (where the separation point is the frequency with the minimum variance) , and the ratio Φ_{Sw} based on the ratio of the wind sea and swell peak frequencies (Van Maris, 2018). The relative swell variance is given by:

$$M_{Sw} = \frac{m_{0,swell}}{m_{0,swell} + m_{0,sea}} \tag{6}$$

and the relative swell peak frequency is defined as.

$$\Phi_{Sw} = \frac{f_{p,swell}}{f_{p,swell} + f_{p,sea}} \tag{7}$$

An overview of all SWASH simulations carried out is given in Table 1. Here $L_{1/3}$ is the local wave length computed from $T_{1/3}$, and $T_{1/3}$ is the mean of the periods corresponding to the 1/3 highest waves.

Tab. 1: Summary SWASH simulation conditions

Simulation	Relative depth	Wave steepness	Relative swell variance	Relative swell peak frequency
	$d/L_{1/3}$ or d/L [-]	$H_{1/3,loc}/L_{1/3}$ [-]	M_{SW} [-]	Φ_{SW}
IJmuiden case	0.64	0.057	0.02	0.62
Validation SWASH	0.123	0.036-0.092	-	-
Regular wave	0.07-0.8	0 – 0.11	-	-
Unimodal spectrum	0.18-0.77	0-0.06	-	-
Bimodal spectrum	0.26-0.48	0.017-0.045	0 – 0.25	0.4-0.75

4 Results

4.1 Pressure distribution

Figure 4 shows typical vertical pressure distributions for the different design formulae. The pressure is made non-dimensional by dividing by (½*gd*) and the vertical axis is made non-dimensional (partial depth) by dividing by depth *d*.

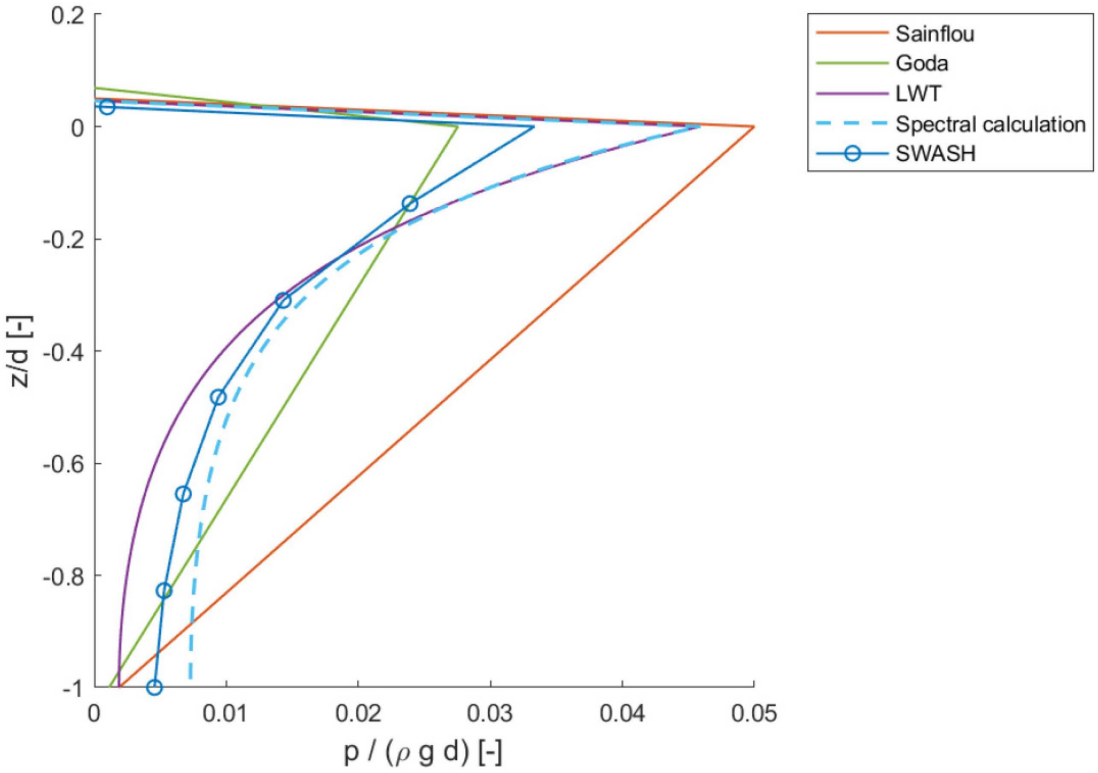

Fig. 4. Example of pressure profiles obtained using different design methods for the IJmuiden loading case (source: Van Maris, 2018).

For design guidelines and linear wave theory $H_{1/3}$ and $T_{1/3}$ are used as input parameters. The spectral calculation is applied for F_{m0}. For the SWASH, the pressure distribution that corresponds with $F_{1/3}$ is plotted.

From this example it can be observed how the pressure distributions differ between the design methods. The Sainflou and Goda formulae give a simplified linear pressure distribution below SWL. The LWT gives a more accurate estimation of the pressure distribution of the SWASH simulation, but underestimates in greater partial depth. The spectral calculation method accounts for the swell component. It can also be seen that the Sainflou methods overestimates the pressures in comparison with the other methods.

4.2 Irregular waves – unimodal spectrum

This paragraph compares the characteristic horizontal wave force in an irregular wave field from the various design methods. The characteristics value refers to the value with a probability of exceedance of 0.135 and corresponds to the significant wave height $H_{1/3}$ and significant wave force $F_{1/3}$. In Figure 5 the design guidelines and spectral calculation method are compared with the SWASH results for various unimodal wave spectra with different wave steepness and relative depth. The design guidelines are applied with $H_{1/3}$ and $T_{1/3}$. On the vertical axis, the $F_{1/3}$ is made non-dimensional by dividing by ($\frac{1}{2}gd^2$). The wave force is plotted for various relative depths $d/L_{1/3}$ (indicated by the different colors) over the wave steepness $H_{1/3,loc}/L_{1/3}$ on the x-axis. The following observations and accompanying explanations are made:

- The SWASH simulations present a linear increase in wave force for an increase in wave steepness.
- Sainflou overestimates the force of the SWASH simulations for an increasing wave steepness and an increasing depth up to a value of more than 2. The increase due the wave steepness is explained by the incorporation of h_0, which accounts for second order components. The increase due the relative depth is explained by the linear pressure distribution which is a rough simplification of the actual pressure distribution, especially in greater depths.
- Goda underestimates the forces for shallow waters ($d/L_{1/3}$ = 0.18 and $d/L_{1/3}$ = 0.33) by approximately 15% compared to the SWASH and spectral computation. In deeper waters, Goda gives an overestimation of the force of 5% to 20%. The overestimation of the horizontal wave force in deeper waters is, similar as Sainflou, due to the linear pressure distribution which is a rough simplification (Note that Goda is known as a conservative formula; which is not the case for shallow water).
- Linear wave theory gives a good representation of the forces simulated by SWASH, except for steep waves in intermediate water depth where it gives a small overestimation of about 10%.
- The spectral calculation gives similar results as the LWT. The increase in force for greater depths can be explained by the fact that there is more wave variance in the spectral domain located below the design wave frequency used in the LWT. This makes the spectral method compared to the LWT more accurate to the presence of low frequency energy. In deeper waters, these low frequencies weigh relatively heavier than in shallow waters, making the LWT negatively biased (= conservative) for an increasing depth.

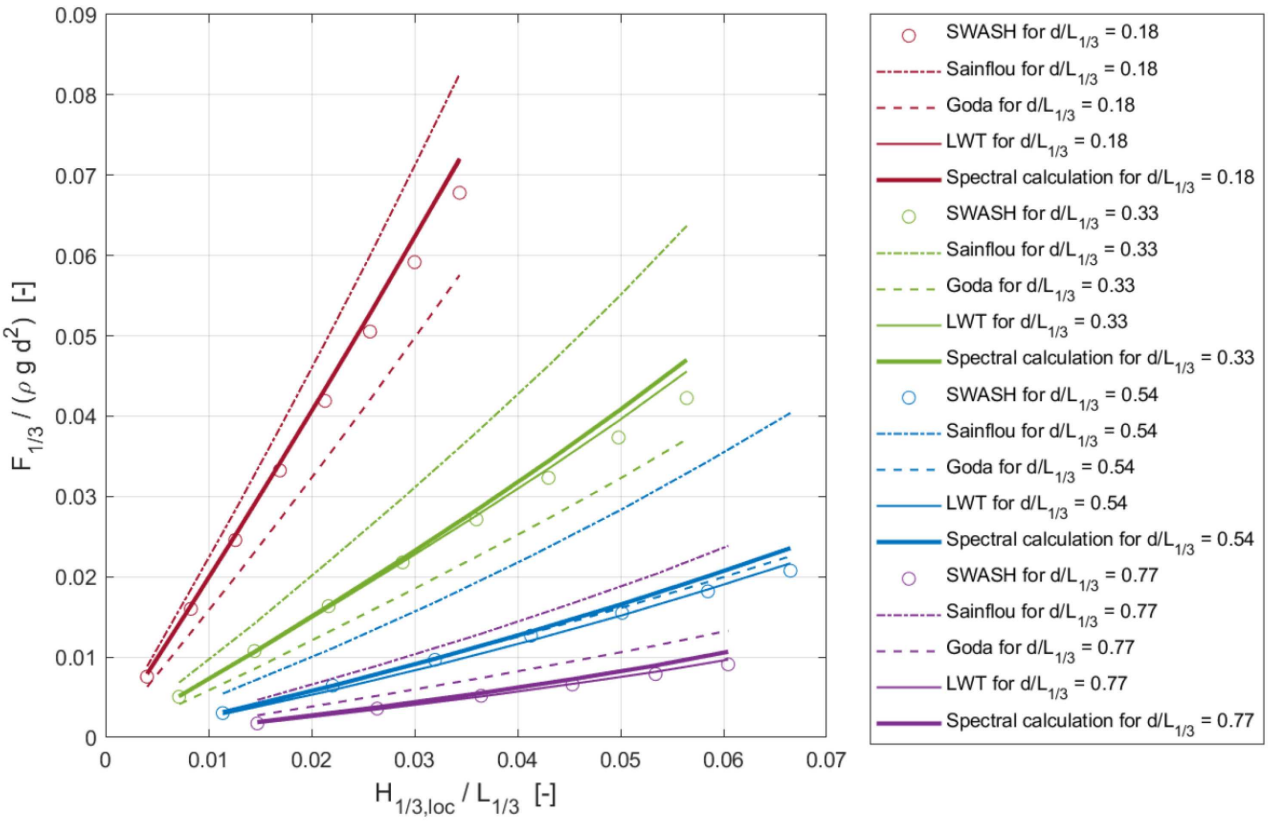

Fig. 5: Non dimensional significant force $F_{1/3}$ for an increasing wave steepness plotted for various relative depths. Numerical results are indicated by dots and the continuous lines presents the analytical solutions of design guidelines (source: Van Maris, 2018).

4.3 Irregular wave – bimodal spectrum

Three simulations in SWASH are carried out by simulating a swell component, a wind sea component and a bimodal spectrum as a sum of these components. Table 2 presents an overview of the characteristics and results of these three simulations. The first and second column show the characteristics of the quantity under consideration and the corresponding unit. The third and fourth column present the values for the simulated swell and wind component respectively. The column with

the header "superposition" applies a linear superposition of the swell and wind sea components. The spectral moments m_0 are summed linearly and consequently the wave height H_{m0} are summed quadratically. With the assumption that the characteristic wave force present in the sea state is linear related to the energy in the wave field, linear superposition on the forces is applied. In the sixth column, the results from the results simulated bimodal spectrum are presented. The last column indicates the relative increase due to the presence of the swell peak, with respect to the wind sea spectrum. Design formulae and LWT are calculated with $H_{1/3}$ and $T_{1/3}$.
From the table, the following observations are made:

- Superposition of H_{m0} (or m_0) results in the same values as observed in the bimodal spectrum.
- For the simulated swell components (relatively shallow water with $d/L<0.33$), all design methods present quite accurate results. In deeper water, the design methods present overestimations of approximately 10% (Goda, LWT, spectral calculation) or 100% (Sainflou). These observations are similar to those found in Figure 5.
- Linear superposition of m_0 of the swell and wind sea component by all design methods results in an overestimation of the design force present in a bimodal wave spectrum. Goda, spectral calculation and SWASH overestimates the force compared to the force calculated for the bimodal spectrum.
- Compared to SWASH, the LWT and Goda give accurate estimation of the horizontal wave force induced by the bimodal spectrum. The spectral calculation method overestimates with approximately 10% and Sainflou with approximately 100%.
- Due to swell, the significant horizontal wave force increases by 8.41% while the wave variance m_0, significant wave height H_{m0} and significant wave period $T_{1/3}$ only increase with 2.1%, 1.3% and 0.82% respectively. The spectral wave period increases with 6.7% under the influence of the swell component. This comes close to the increase in horizontal wave force by SWASH. $F_{1/3,spectral}$ accounts for a similar increase as $F_{1/3,SWASH}$.

Tab. 2: Characteristics of the wave field of the decomposed bimodal wave spectrum, compared with the values of superposition and the original bimodal spectrum (source: Van Maris, 2018)

Symbol	Unit	Swell component	Wind sea component	Superposition	Bimodal spectrum	Increase due to swell [%]
m_0	[m^2]	0.008	0.0334	0.342	0.343	2.1
m_{-1}	[sm^2]	0.099	1.664		1.775	6.7
H_{m0}	[m]	0.36	2.31	2.34	2.34	1.3
$H_{m0}/L(T_{m-10})$	[-]	0.0023	0.0598		0.0566	-5
T_p	[s]	12.80	5.00	-	5.00	0
$H_{1/3}$	[s]	12.44	4.90	-	4.94	0.8
T_{m-10}	[s]	12.37	4.98		5.17	3.8
$F_{1/3,Sainflou}$	[kN/m]	32.34	144.17	176.51	146.12	1.6
$F_{1/3,Goda}$	[kN/m]	27.23	81.22	108.45	82.41	1.5
$F_{1/3,LWT}$	[kN/m]	30.78	78.27	109.05	79.43	1.5
$F_{m0,spectral}$	[kN/m]	29.31	80.97	110.28	87.15	7.8
$F_{1/3,SWASH}$	[kN/m]	28.05	72.79	100.84	78.91	8.4

Based on these observations it can be concluded that the linear superposition of the SWASH calculated swell and wind force does not result in the wave force induced by a bimodal spectrum. Neither does this seem to work for the design guidelines, since a rough overestimation of the force is established. There is, however, a distinct increase due the swell component, as the increase in horizontal wave force is out of proportion with the increase in wave variance. The extent of this increase in force is not clearly indicated by the wave characteristics under consideration. Goda and the LWT both give here an accurate estimation of the wave force of the bimodal spectrum. This surprising result, however, seems to be due to a coincidental cancellation of an overestimation of the wind sea component and an underestimation of the swell component. The spectral calculation provides a stable (over)estimation of the SWASH force.

4.4 Relative bimodal force

Up to now, the influence of a swell component is quantified for one sea state. This paragraph addresses the influence of the relative swell parameter M_{Sw} for different sea states. Due to the small influence of the relative peak frequency Φ_{Sw}, this parameter is kept constant (Φ_{Sw} = 0.6) throughout the following simulations. It was already observed that as the swell component increases, the values of $T_{1/3}$ and $H_{1/3}$ are increasing as well, leading to a decrease in wave steepness (increase in L is dominant over increase in H) and a decrease in relative depth. Here, it is aimed that the inclusion of a swell component is not influencing the relative depth and wave steepness. Since it was already seen that the design formulae do not take account the swell component (accurately), only the spectral calculation method is compared with the SWASH results. Furthermore, a new parameter is introduced to define the relative increase in force for a bimodal wave spectrum (Van Maris, 2018):

$$\Delta F_{bi,1/3} = \frac{F_{bi,1/3} - F_{uni,1/3}}{F_{uni,1/3}} \tag{8}$$

In Figure 6, $\Delta F_{bi,1/3}$ is plotted for an increasing relative swell variance M_{Sw} for different sea states. The sea states of the simulations vary in wave steepness $H_{loc,1/3}/L_{1/3}$ indicated by the markers (circles, triangles, squares), and relative depth $d/L_{1/3}$ indicated by the marker type and color. The force estimation by SWASH (markers) is compared with the force estimation by the spectral calculation method (lines).

From the figure the following observations are made:

- The SWASH results show an increase in ΔFbi,1/3, for an increasing relative swell variance MSw.
- Fbi,1/3 shows a strong correlation with relative depth d/L1/3 and no clear correlation with wave steepness Hloc,1/3/L1/3.
- The spectral calculation method gives roughly an accurate estimation for different values of relative depth and wave steepness. However, the spectral calculation method is presenting an overestimation of up to 15% in deeper water and an underestimation of about 20% in shallow water compared to those found by SWASH.

5 Conclusions

For the simplified case of a vertical wall on a flat sea bed (no berm) the following conclusions are made for non-breaking wave loads of gentle waves (steepness lower than 0.03). In the case wave conditions are described by a unimodal wave spectrum, the Sainflou formula is too conservative. The formula of Goda is more accurate, but provides underestimations of about 10% in intermediate water depth. As an alternative, the linear wave theory is an accurate design method for gentle waves in a wide range of relative depths.

When wave conditions by a bimodal spectrum are considered, the influence of swell on the wave force can be considerable. Since wave characteristics ($H_{1/3}$ and $T_{1/3}$) do not distinguish a swell component, traditional design guidelines based on wave characteristics of unimodal spectra may underestimate the wave force. This underestimation is depended on the relative depth and the relative variance of the swell component. A spectral calculation method in which the complete wave spectrum is translated to a force spectrum is an accurate design method for the estimation of non-breaking wave loads on vertical walls.

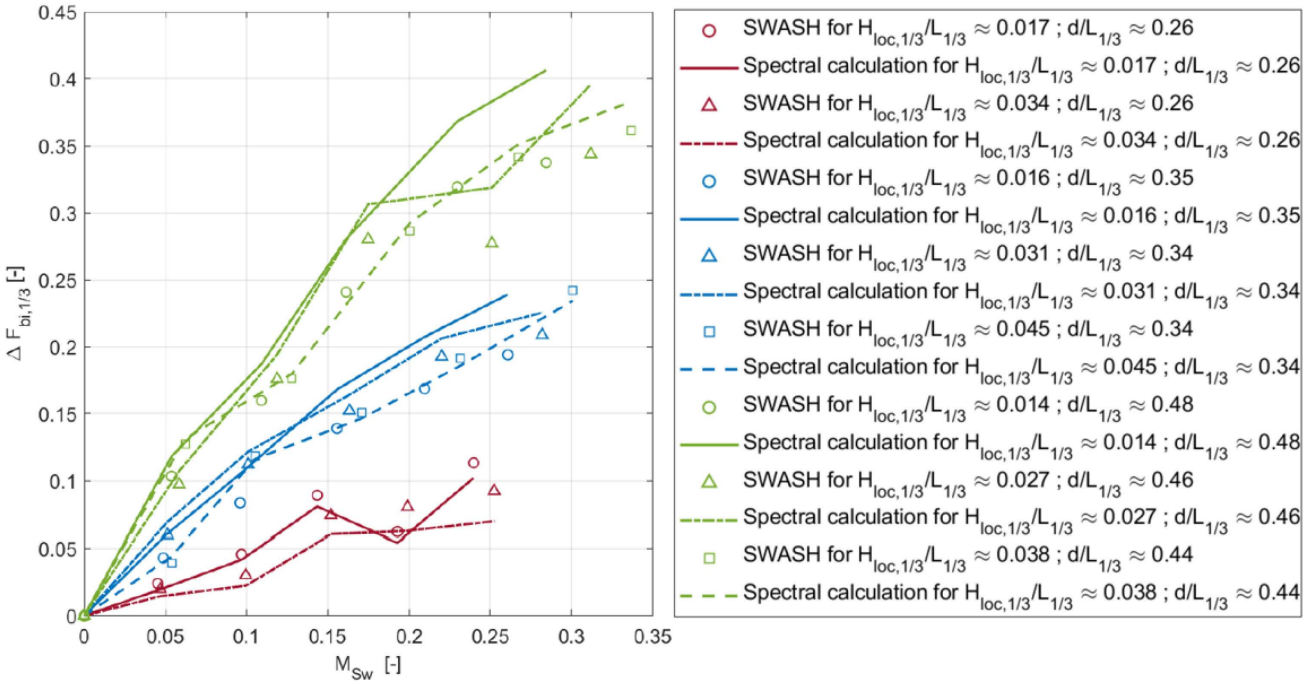

Fig. 6: Relative increase in force for a bimodal spectra, indicated for different relative swell variance, wave steepness and relative depth (source: Van Maris, 2018).

References

CERC, 1984: Shore Protection Manual, Coastal Engineering Research Station, revised edition.

Goda, Y., 1974: A new method of wave pressure calculation for the design of composite breakwaters. Proceeding of 14th International Conference on Coastal Engineering, 14:1702–1720.

Gurhan, G. and D. Unsalan, 2005: A comparative study of the first and second order theories and Goda's formula for wave-induced pressure on a vertical breakwater with irregular waves. Ocean Engineering, 32(17-18):2182–2194.

Hasselmann, K., et al., 1973: Measurements of Wind-Wave Growth and Swell Decay during the Joint North Sea Wave Project (JONSWAP). Ergnzungsheft zur Deutschen Hydrographischen Zeitschrift Reihe, A(8)(8 0):p.95.

Holthuijsen, L.H., 2007: Waves in oceanic and coastal waters. Cambridge Univerisity Press, 387 pp.

Sainflou, M., 1928: Essai sur les diques maritimes verticales. Technical report, Paris.

TAW, 2003 Leidraad Kunstwerken. Rijkswaterstaat, Delft.

Tuin, H.G., H. Voortman, T. Wijdense, W. Van der Stelt, D. Van Goolen, P. Van Lierop, and L. Lous, 2018: Design of roller gates of the lock of Amsterdam using a transformation of the wave spectrum in a frictional force spectrum. PIANC world congress 2018.

Van Maris, B.E., 2018: Wave loads on vertical walls. Validation of design methods for non-breaking waves of bimodal spectra. MSc thesis Delft University of Technology.

Van Vledder, G.Ph., 2018: A hybrid method to combine wave penetration and local wave growth in large harbor basins. Proc. 36th Int. Conf. on Coastal Engineering, Baltimore, MA, USA.

Wiegel, R.L., 1964: Oceanographical Engineering. Berkeley, California: Pentice-Hall International.

Zijlema,M., G.S. Stelling, and P.B. Smit, 2011. SWASH: An operational public domain code for simulating wave fields and rapidly varied flows in coastal waters. Coastal Engineering, 58(10):992–1012.